

## Supplementary Information

### **Synthesis and Electrochemical Studies of Novel Phosphite Based Layered Cathodes for Li-ion Batteries**

A. Shahul Hameed<sup>a</sup>, M. V. Reddy<sup>\*bc</sup>, Nirjhar Sarkar<sup>b</sup>, B. V. R. Chowdari<sup>b</sup> and Jagadese J. Vittal<sup>\*a</sup>

<sup>a</sup>Department of Chemistry, National University of Singapore, Singapore 117543.

<sup>b</sup>Advanced batteries lab, Department of Physics, National University of Singapore, Singapore 117542.

<sup>c</sup>Department of Materials Science and Engineering, National University of Singapore, Singapore 117575.

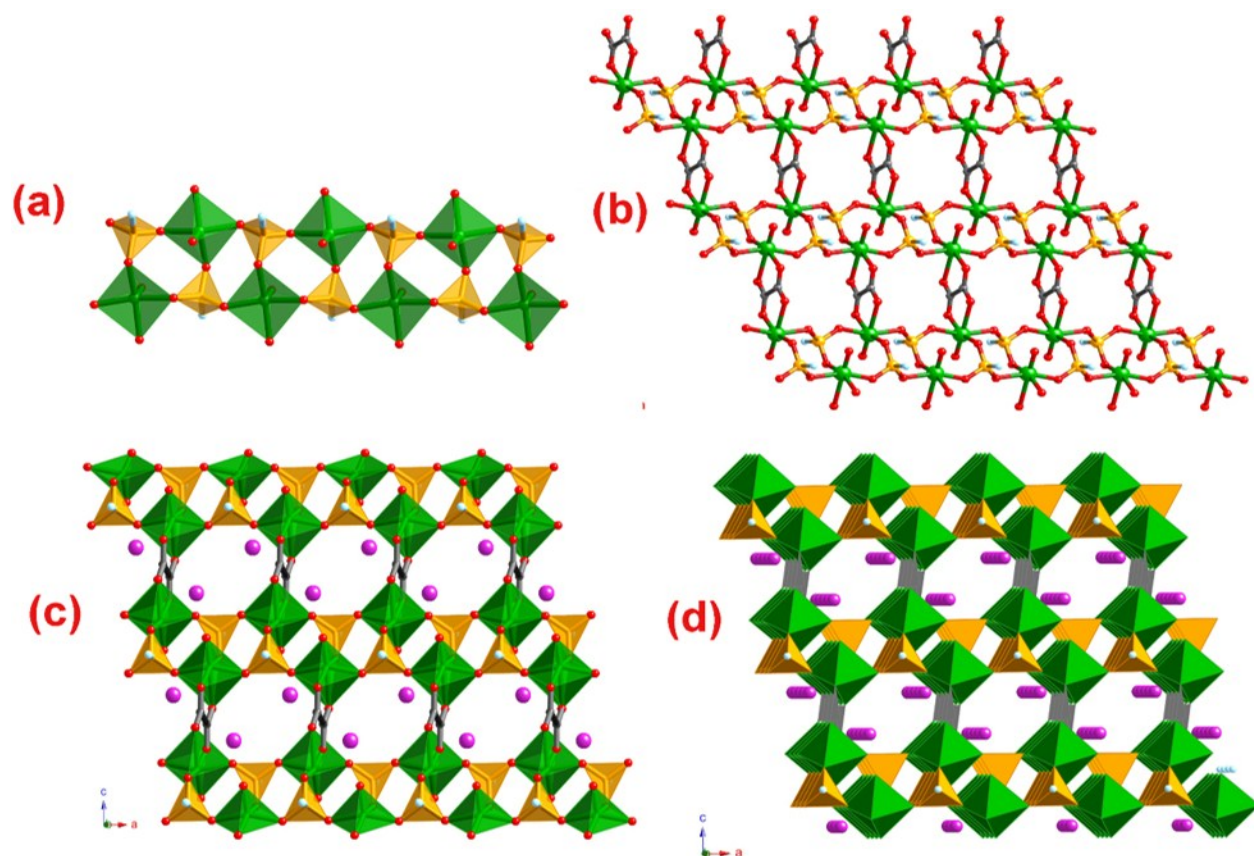


**Fig. S1.** Crystal structure of  $\text{Na}_2[(\text{VO})_2(\text{HPO}_3)_2(\text{C}_2\text{O}_4)] \cdot 2\text{H}_2\text{O}$ ; (a) View of  $\text{VOHPO}_3$  chains; (b and c) View of  $[(\text{VO})_2(\text{HPO}_3)_2(\text{C}_2\text{O}_4)]$  layer along (01-1) plane formed by interlinking of  $\text{VOHPO}_3$  chains by oxalate ligands; (b) ball and stick model and (c) polyhedral model with Na ions in the channel; (d) Stacking of the anionic layers along  $c$ -axis result in the layered structure with  $\text{Na}^+$  ions between the layers. The water molecules present in between layers are not shown for clarity

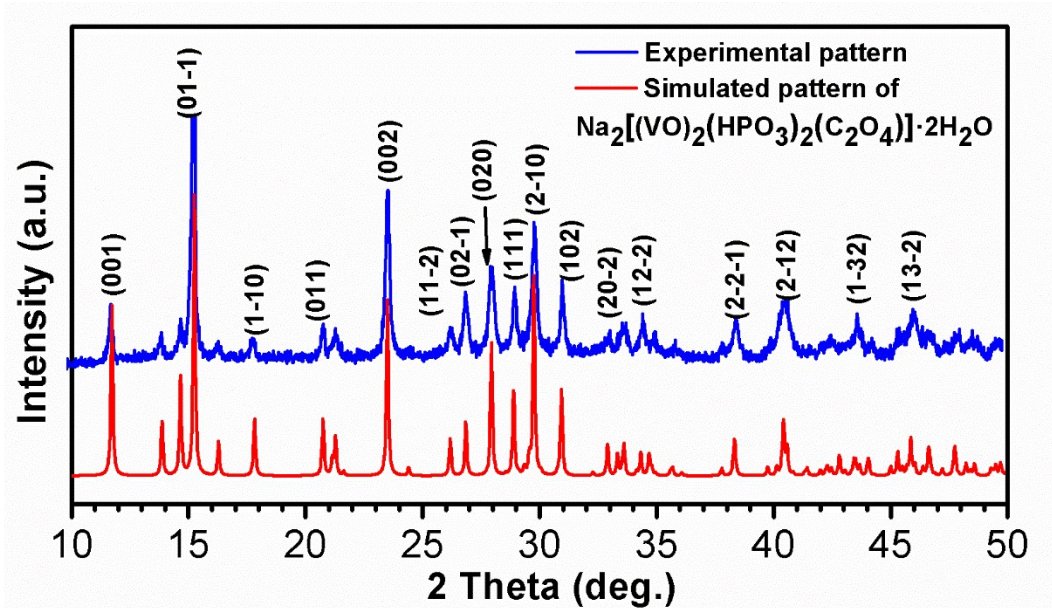


**Fig. S2.** Comparison of PXRd pattern of bulk  $\text{Na}_2[(\text{VO})_2(\text{HPO}_3)_2(\text{C}_2\text{O}_4)] \cdot 2\text{H}_2\text{O}$  powder (red) with its simulated pattern (blue)

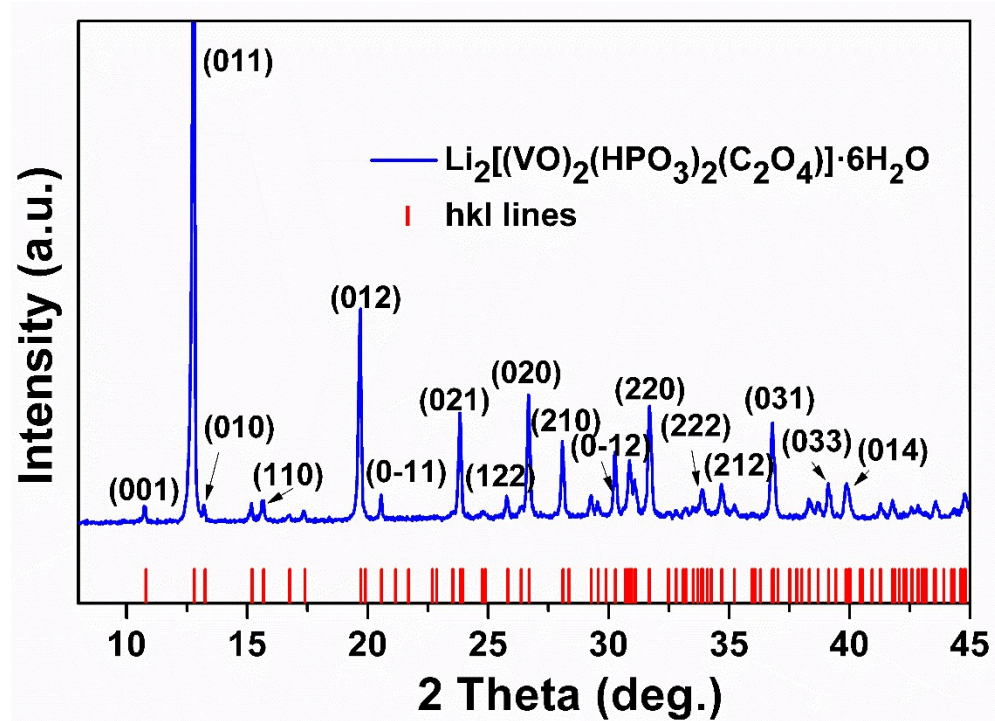


**Fig. S3.** PXRD pattern of  $\text{Li}_2[(\text{VO})_2(\text{HPO}_3)_2(\text{C}_2\text{O}_4)] \cdot 6\text{H}_2\text{O}$  powder (blue) compared with its literature report (hkl lines are indicated in red)

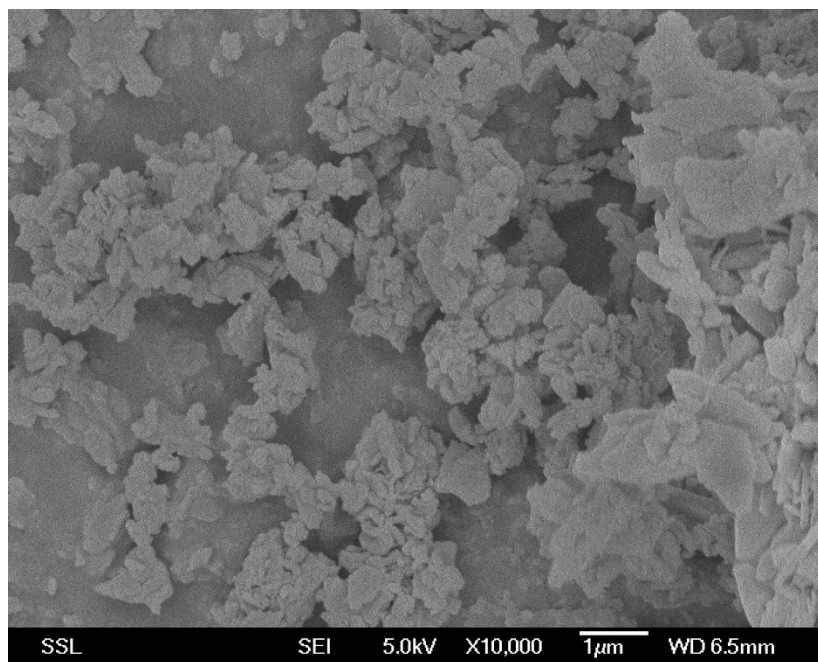


**Fig. S4.** SEM micrograph of rGO/Li<sub>2</sub>[(VO)<sub>2</sub>(HPO<sub>3</sub>)<sub>2</sub>(C<sub>2</sub>O<sub>4</sub>)]·6H<sub>2</sub>O composite.



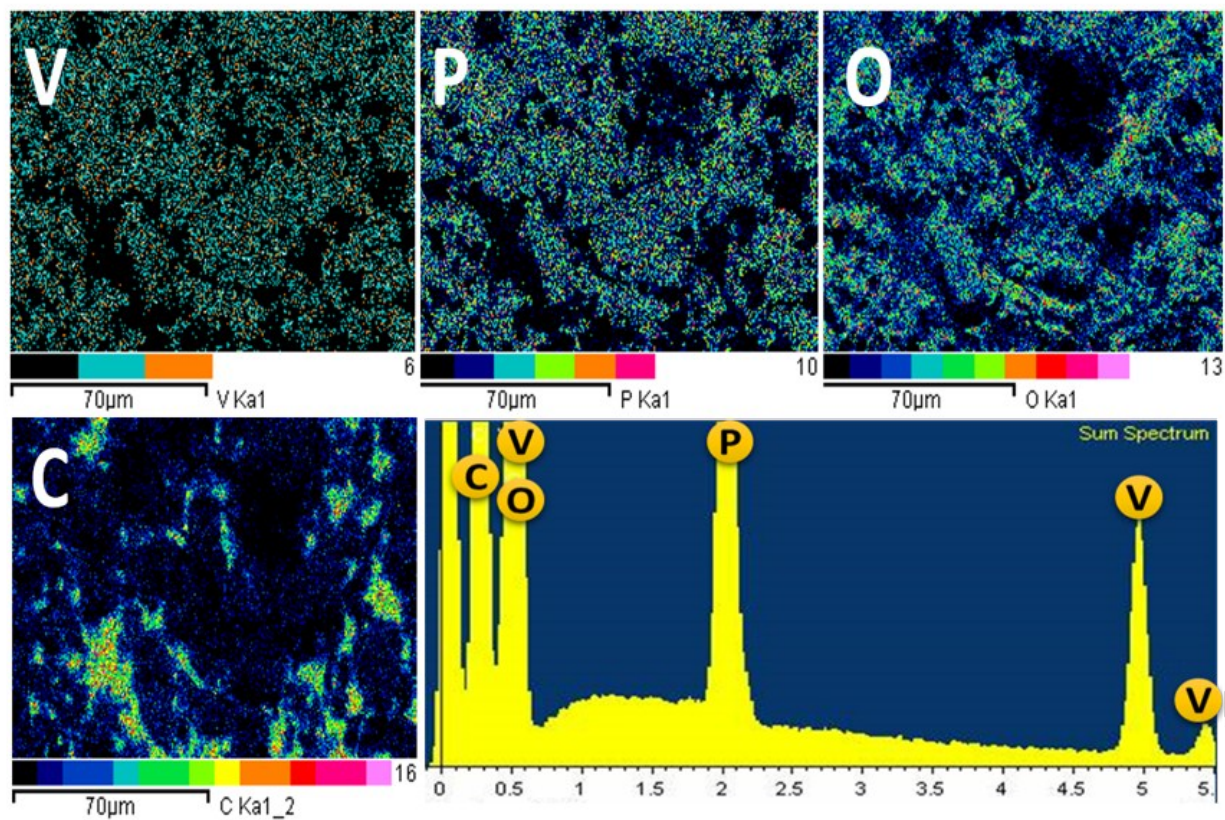


**Fig. S5.** EDX element mapping of  $\text{Li}_2[(\text{VO})_2(\text{HPO}_3)_2(\text{C}_2\text{O}_4)] \cdot 6\text{H}_2\text{O}$  for V, P, C and O along with the EDX spectrum

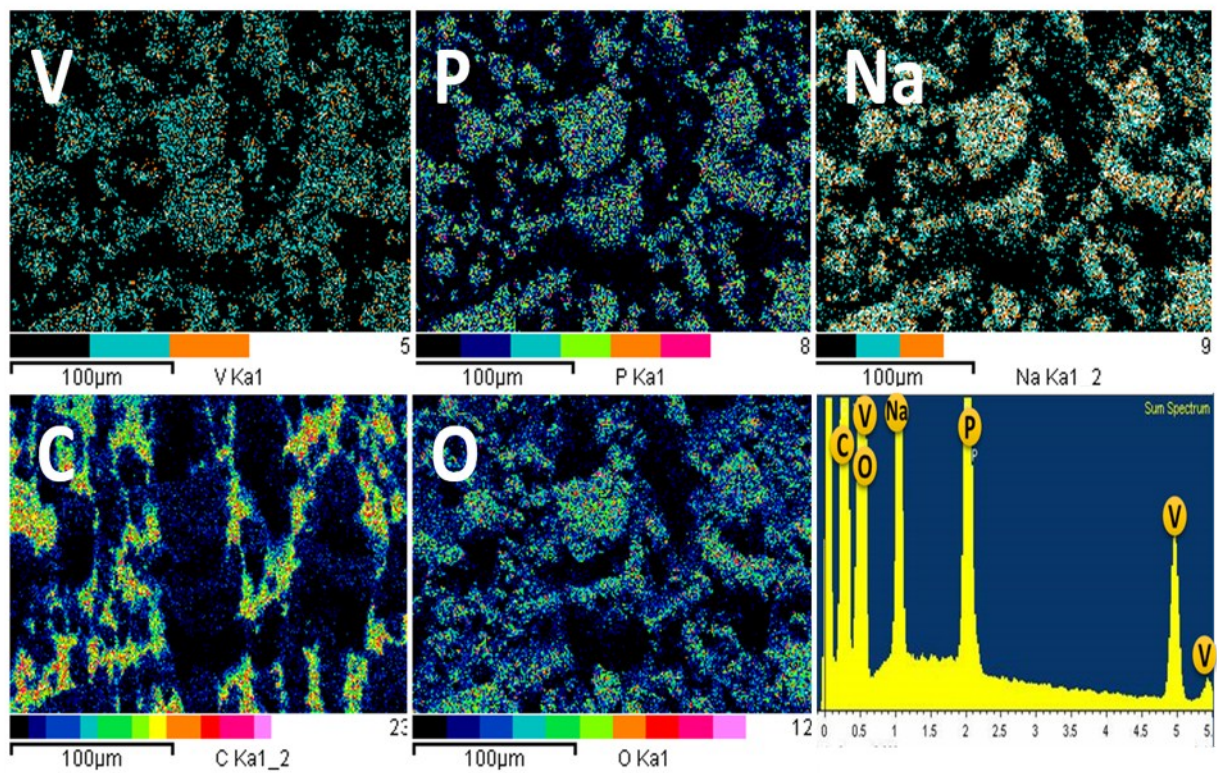


**Fig. S6.** EDX element mapping of  $\text{Na}_2[(\text{VO})_2(\text{HPO}_3)_2(\text{C}_2\text{O}_4)] \cdot 2\text{H}_2\text{O}$  for V, P, Na, C and O along with the EDX spectrum



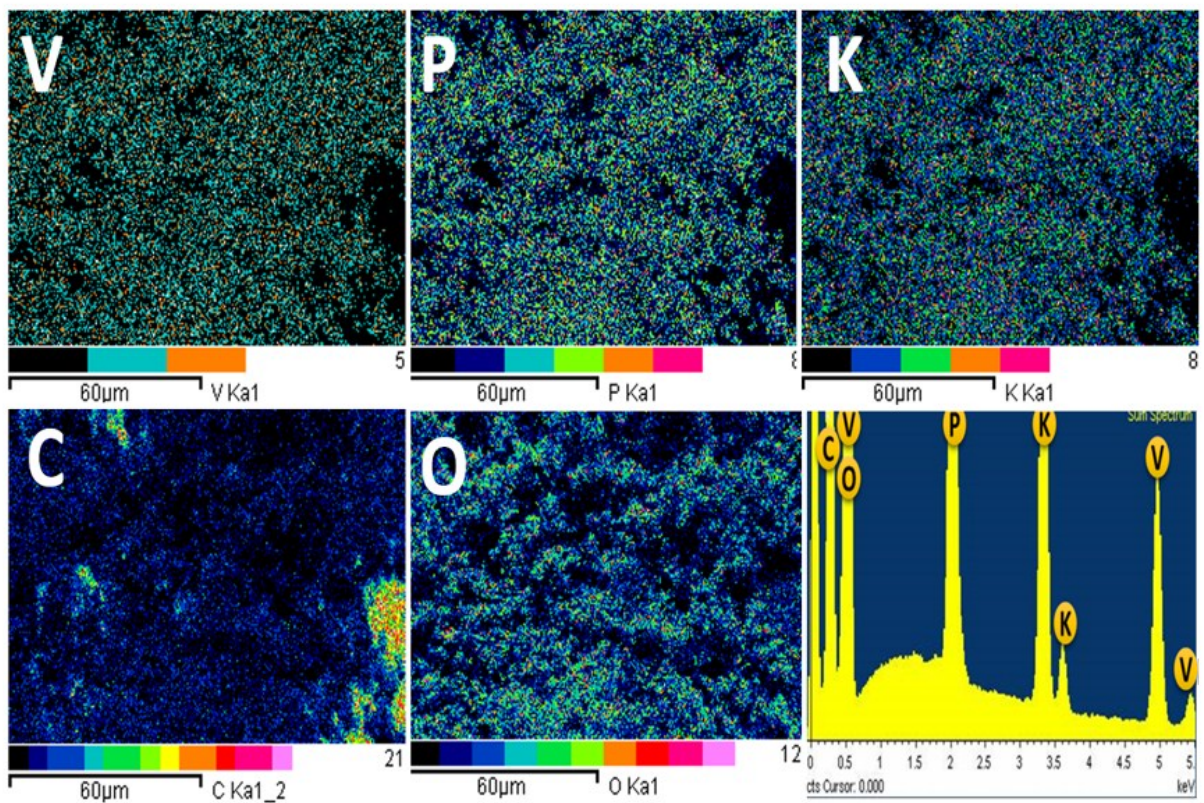


**Fig. S7.** EDX element mapping of  $K_2[(VO)_2(HPO_3)_2(C_2O_4)] \cdot 3H_2O$  for V, P, K, C and O along with the EDX spectrum



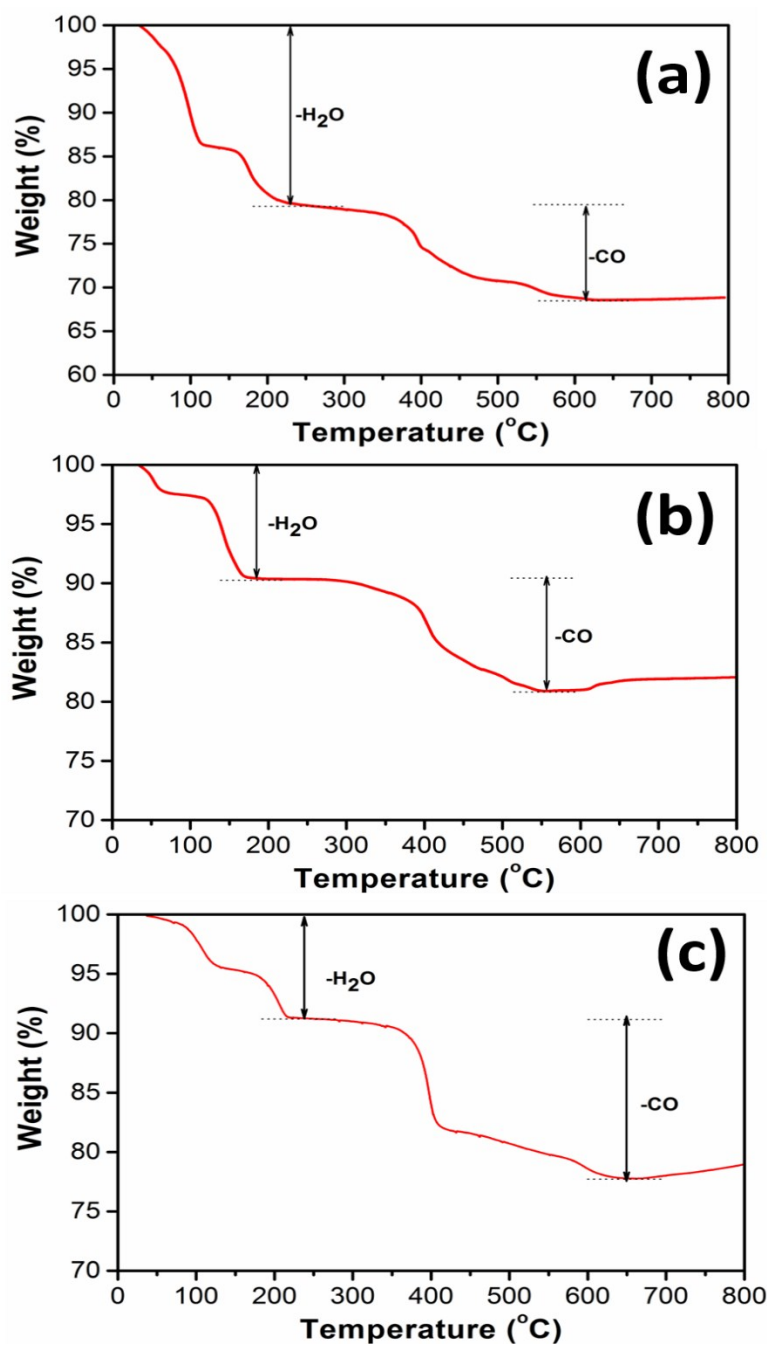


**Fig. S8.** Thermogravimetric analysis (TGA) of (a)  $\text{Li}_2[(\text{VO})_2(\text{HPO}_3)_2(\text{C}_2\text{O}_4)] \cdot 6\text{H}_2\text{O}$ ; (b)  $\text{K}_2[(\text{VO})_2(\text{HPO}_3)_2(\text{C}_2\text{O}_4)] \cdot 3\text{H}_2\text{O}$  and (c)  $\text{Na}_2[(\text{VO})_2(\text{HPO}_3)_2(\text{C}_2\text{O}_4)] \cdot 2\text{H}_2\text{O}$  recorded in  $\text{N}_2$  atmosphere at a heating rate of  $5\text{ }^\circ\text{C min}^{-1}$

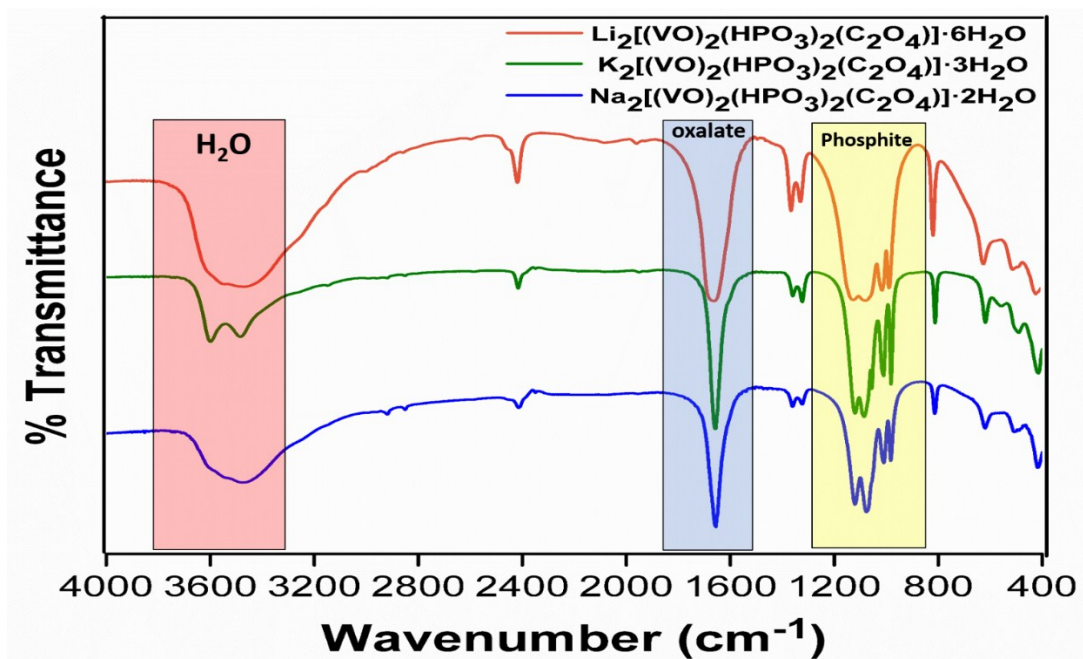


**Fig. S9.** Infra Red spectra of  $\text{Li}_2[(\text{VO})_2(\text{HPO}_3)_2(\text{C}_2\text{O}_4)] \cdot 6\text{H}_2\text{O}$ ,  $\text{K}_2[(\text{VO})_2(\text{HPO}_3)_2(\text{C}_2\text{O}_4)] \cdot 3\text{H}_2\text{O}$  and  $\text{Na}_2[(\text{VO})_2(\text{HPO}_3)_2(\text{C}_2\text{O}_4)] \cdot 2\text{H}_2\text{O}$

